

# Analysis of various dosimetric parameters using multiple detectors in the cyberknife® robotic radiosurgery system

M. Manavalan<sup>1\*</sup>, M. Duraisamy<sup>2</sup>, V. Subramani<sup>3</sup>, H.F. Godson<sup>4</sup>,  
G. Krishnan<sup>5</sup>, M. Venkataraman<sup>6</sup>, T. Ganesh<sup>7</sup>

<sup>1</sup>Research and Development Centre, Bharathiar University, Coimbatore, India

<sup>2</sup>Medanta The Medicity Hospital, Gurgaon, India

<sup>3</sup>Brunei National Cancer Centre, Brunei

<sup>4</sup>Department of Radiotherapy, Christian Medical College, Vellore, India

<sup>5</sup>Department of Radiation Oncology, Apollo Proton Cancer Centre, Chennai, India

<sup>6</sup>Department of Radiation Oncology, Apollo Speciality Hospitals, Chennai, India

<sup>7</sup>Manipal Hospitals Dwarka, India

## ABSTRACT

**Background:** Accurate dosimetry in CyberKnife® is challenging because of the unavailability of suitable detectors to satisfy all the criteria of small-field dosimetry. In this work, eight different small-field detectors from PTW and IBA Dosimetry were used to determine the dosimetric parameters for twelve fixed collimators in the CyberKnife® radiosurgery system. The scope of this work was to assist medical physicists in detector selection in small-field dosimetry. **Materials and Methods:** Dosimetric parameters such as the surface dose ( $D_s$ ), dose buildup ( $D_B$ ), percentage dose at 100 mm ( $D_{100}$ ), percentage dose at 200 mm ( $D_{200}$ ), depth of dose maximum ( $D_{max}$ ), and total scatter factor ( $S_{cp}$ ) were compared and analyzed from the acquired Percentage Depth Dose (PDD). **Results:** Large variations in  $D_s$  were observed with different detectors for smaller collimator sizes. On analyzing the dose buildup, considerable differences were observed with all detectors from the surface to 6 mm depth for the smallest cone of 5 mm diameter. The  $D_{100}$  and  $D_{200}$  values obtained using ion chambers were higher than those using diodes, likely due to the volume averaging effect. The depth of dose maximum was found to increase with increase in the field size for most of the detectors. Considerable variation in  $S_{cp}$  was noticed with all detectors in smaller field ranges. **Conclusion:** For small fields, the selection of detector is crucial, and awareness of the advantages, disadvantages and limitations of the detectors used is crucial. As in absolute dosimetry, the relative dosimetry in small fields is challenging and requires further studies and recommendations.

**Keywords:** CyberKnife®, detectors, PinPoint chamber, diodes, PDD, small field dosimetry.

## ► Original article

### \*Corresponding authors:

M. Manavalan, Ph.D.,

### E-mail:

[emailmuthukumaran@gmail.com](mailto:emailmuthukumaran@gmail.com)

Revised: August 2019

Accepted: September 2019

Int. J. Radiat. Res., July 2020;  
18(3): 437-447

DOI: 10.18869/acadpub.ijrr.18.3.437

## INTRODUCTION

The CyberKnife® system has been used in the treatment of stereotactic radiotherapy (SRS) with submillimeter positional accuracy<sup>(1)</sup>. In this system, the linear accelerator without a flattening filter is mounted on a robotic arm. The

iris collimators incorporated in the CyberKnife® system facilitates a variable aperture to achieve different field sizes similar to cones without changing the collimators during treatment<sup>(2)</sup>. Two different types of collimators, fixed (also referred to as cone) and iris collimators, are used to generate small fields in CyberKnife®.

The iris collimator allows variation of the radiation field size during treatment and can reduce the peripheral dose, unlike fixed collimators. The accurate dose measurements of small fields in CyberKnife® is a challenging task due to electronic disequilibrium, steep dose gradients and source occlusion (3-5) Furthermore, the directional and energy response of detectors influence the dosimetric measurements of small fields (6,7). Additionally, volume averaging and perturbation are caused by the finite size of the active volume of the detector and non-water equivalence materials (8,9).

Because the detectors used for conventional dosimetry cannot be used due to finite collimator opening in CyberKnife®, dedicated dosimeters are vital for small-field dose measurements. Ideally, a dosimeter should have a small water equivalent sensitive volume that allows high positional accuracy with a negligible dose rate, energy and directional dependence. Currently, there are no single detectors that are ideal for small-field dosimetry (4). With technological advancements, many detectors have been introduced to address the aforementioned issues; however these dosimeters have their own limitations. The comparison of several active detectors carried out by Morin et al. indicates that the currently available detectors have limitations in the dose measurements of small fields less than 20 mm in diameter. Additionally, a multicenter study has highlighted the variation in dosimetric parameters of CyberKnife® acquired with different detectors (8). Keivan *et al.* evaluated the dosimetric characteristics of diodes and ionization chambers in small-field photon beams (10). Francescon *et al.* reported the variability in the total scatter factors with different detectors for the smallest collimators of the CyberKnife® system. Many studies have summarized the challenges and limitations using different detectors in small-field dosimetry.

An attempt has been made to perform dosimetric measurements in CyberKnife® treatment units using eight different detectors procured from two different vendors. Dosimetric parameters, such as the surface dose [ $D_s$ ], dose buildup [ $D_B$ ], percentage dose at 100 mm [ $D_{100}$ ],

percentage dose at 200 mm [ $D_{200}$ ], depth of dose maximum [ $D_{max}$ ], and total scatter factor [ $S_{cp}$ ], were evaluated from the obtained PDDs. We aimed to evaluate the accuracy in the measurement of the aforementioned dosimetric parameters using eight different detectors and emphasize the need to perform relative measurement in small fields using more than one detector (11). The study not only provides invaluable data but also helps to clarify the challenges involved in relative measurements in small fields. This study will be useful to select the appropriate detector for relative measurements in CyberKnife® and will assist medical physicists in understanding how different small-field detectors show a significant difference in the measured parameters. The impact due to different dosimetric parameters with various detectors in the dose calculation is not discussed in this study, but the impact these differences would have in dose calculation can be predicted.

## MATERIALS AND METHODS

### Treatment unit

Dosimetric measurements were performed using the G4 CyberKnife® (Accuray Inc., Sunnyvale, CA, USA) treatment unit. This system has an X-band linear accelerator with a nominal energy of 6 MV mounted on a robotic manipulator with 6 degrees of freedom. The small fields ranging from 5 mm to 20 mm with an increment of 2.5 mm and 20 mm to 60 mm with an increment of 5 mm at the source-to-axis distance (SAD) of 80 cm can be defined by either a fixed collimator called cones or a variable aperture called the iris collimator. The treatment machine can produce different dose rates, but a nominal dose rate of 800 MU/ min was used in this study. All measurements were performed using fixed collimators for twelve different cones.

### Dosimetric measurement tools

The detectors used in this study were PTW microDiamond, PTW SRS diode, PTW photon diode, PTW electron diode, PTW 31014 pinpoint

ion chamber, Scanditronix photon field diode (PFD), Scanditronix electron diode (EFD) and Scanditronix SRS diode (SFD) detectors. The PTW diodes and microdiamond, as well as the Scanditronix diodes, were positioned vertically to the central axis (CAX) of the beam, while the PTW PinPoint ion chamber was positioned horizontally to the CAX of the beam during measurements. The diodes and microDiamond were operated at 0 volts, and the pinpoint chamber was operated at +400 volts. The detectors were mounted accurately in the water

phantom at its effective point of measurement (EPOM) as provided by the manufacturer. The characteristics of the detectors used in this study are tabulated in table 1. The PTW MP3-M 3D motorized water phantom with a positional accuracy of 0.1 mm was used for data acquisition. The scanning dimension of the MP3-M water phantom is 500 × 500 × 408 mm. PTW MEPHYSTO software version 3.1 was used to control the movements of the detectors in the water phantom and to analyze the acquired data.

Table 1. Technical details of the detectors used in the study.

Detector type	Type of product	Nominal sensitive volume	Design	Reference point	Sensitive volume	Energy response	Outer dimension
PTW photon diode	p-type silicon diode	0.025 mm <sup>3</sup>	Waterproof disk-shaped sensitive volume perpendicular to the beam	2 mm behind the front side	1-mm <sup>2</sup> circle, 2.5-µm thick	<sup>60</sup> Co to 25 MV	Diameter=7 mm, length=47 mm
PTW electron diode	p-type silicon diode	0.03 mm <sup>3</sup>	Waterproof disk-shaped sensitive volume perpendicular to the beam	1 mm behind the front side	1-mm <sup>2</sup> circle, 30-µm thick	6-25 MeV electrons, <sup>60</sup> Co to 25 MV photons	Diameter=7 mm, length=45.5 mm
PTW SRS diode	p-type silicon diode	0.3 mm <sup>3</sup>	Waterproof disk-shaped sensitive volume perpendicular to the beam	1.31 mm from the detector tip	1-mm <sup>2</sup> circle, 250-µm thick	<sup>60</sup> Co to 6 MV photons	Diameter=7 mm, length=45.5 mm
PTW microDiamond	microDiamond type	0.004 mm <sup>3</sup>	Waterproof disk-shaped sensitive volume perpendicular to the beam	1 mm from the detector tip marked by a ring	1.1mm <sup>2</sup> circle, 1-µm thick	100 keV to 25 MV, 6-25 MeV electrons	Diameter=7 mm, length=45.5 mm
PTW PinPoint chamber	Vented cylindrical ion chamber	16 mm <sup>3</sup>	Waterproof, vented, fully guarded and mounted parallel to the beam	On the chamber axis, 2.4 mm from the tip	1.45mm radius, 2.9-mm length	<sup>60</sup> Co to 50 MV	Diameter=4.3 mm, length=5.3 mm
Scanditronix PFD	High-psi semiconductor	0.29 mm <sup>3</sup>	Waterproof disk-shaped sensitive volume perpendicular to the beam	0.5 ± 0.15 mm from the detector tip	2.5-mm diameter, 0.06-mm thick	1-50 MV/ MeV	Diameter=7 mm, length=75 mm
Scanditronix EFD	High-psi semiconductor	0.29 mm <sup>3</sup>	Waterproof disk-shaped sensitive volume perpendicular to the beam	0.45 ± 0.1 mm from the detector tip	2.5-mm diameter, 0.06-mm thick	1-50 MV/ MeV	Diameter=7 mm, length=75 mm
Scanditronix SFD	High-psi semiconductor	0.017 mm <sup>3</sup>	Waterproof disk-shaped sensitive volume perpendicular to the beam	0.5 ± 0.15 mm from the detector tip	0.6-mm diameter, 0.06-mm thick	1-50 MV/ MeV	Diameter=5 mm, length=75 mm

**Experimental setup**

The PDD data were acquired using all the detectors mentioned above for all twelve fixed collimators. The PDDs were acquired by scanning the detectors from the depth of 30 cm to the surface of the water tank in steps of 0.5 mm. The detector was moved from the bottom to the surface of the water to avoid water turbulence during scanning. To assess the setup accuracy of the water phantom, the PDD was measured with a particular detector before performing measurements with other detectors. All PDDs were acquired, keeping the source-to-surface distance of 80 cm.

**Software used for data analysis**

The positional accuracy of the detectors with respect to the central axis of the beam is ensured by measuring two profiles at 1.5-cm and 10-cm depths and is analyzed using Center Check software (PTW, Germany). To characterize the influence of different detectors in small fields, various dosimetric parameters from PDD were analyzed and compared for all detectors using the Data Analysis module in PTW Mephysto software 3.1.

**RESULTS**

**Analysis of the surface dose ( $D_s$ )**

The relative surface dose obtained from the PDD data showed a large variation in all fields with different detectors. The variation in  $D_s$  from the smallest collimator to the largest collimator for various detectors is shown in figure 1. The minimum  $D_s$  measured by the Scanditronix EFD was 34.13% for a 7.5-mm collimator, a value that was 13.4% lower than the average value of  $47.5\% \pm 9.4\%$ , whereas an overestimation of 15% was observed with the PTW microdiamond from the average  $D_s$  value for the same field. Unlike in conventional field sizes, where  $D_s$  increases with the field size, a similar pattern was not observed in these small fields. All the detectors showed a similar pattern of decreasing  $D_s$  with increasing field size ranging from 5 mm to 25 mm, and then  $D_s$

gradually increased to the largest collimated field size of 60 mm. The statistical analysis of  $D_s$  for all collimator sizes is tabulated in table 2.

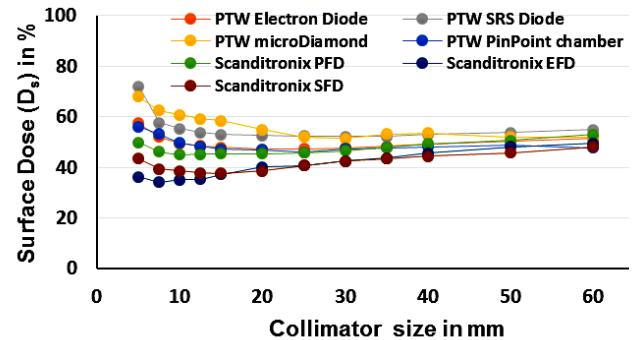


Figure 1. Variation in  $D_s$  (%) measured with different detectors for various collimator sizes.

Table 2. Average detector response, minimum  $D_s$ , maximum  $D_s$  and standard deviation of  $D_s$  with different detectors for various field sizes.

Collimator Size (mm)	Average $D_s$ (%)	Minimum $D_s$ (%)	Maximum $D_s$ (%)	Standard Deviation (%)
5	51.8	36.2	62.9	10.5
7.5	47.5	34.1	57.6	9.4
10	45.9	34.0	55.3	8.5
12.5	45.1	34.2	53.7	7.7
15	45.1	35.5	53.0	6.8
20	45.2	36.5	52.5	6.0
25	46.0	38.6	52.4	5.0
30	46.6	40.2	52.1	4.2
35	47.6	43.3	52.5	3.5
40	48.6	44.9	52.9	3.0
50	49.7	46.2	53.6	2.7
60	51.2	47.7	54.9	2.4

**Analysis of the dose buildup region [ $D_B$ ]**

In this study, the doses in the buildup region were measured for twelve fixed collimators with eight detectors. However, detailed analysis in the dose buildup region was carried out for the smallest collimator size (5 mm), a mid-range collimator (20 mm), and the largest collimator (60 mm). Similar to  $D_s$ , where a large difference is observed with different detectors for the 5-mm collimator, we observed a large difference in the dose buildup for a small collimator size (figure 2). Regarding the 5-mm collimator, the Scanditronix EFD showed a lower dose gradient in the buildup region.

At 1 mm, a considerable dose difference of nearly 50% was observed between the PTW photon diode and Scanditronix EFD. At 2, 3, and 4 mm, this difference decreased to nearly 30%, 20% and 12%, respectively. The PinPoint detector showed a steep dose gradient in the buildup region, while the PTW photon diode showed a low dose gradient. For the 20-mm collimator, all the detectors showed a gradual increase in the dose buildup (figure 3). For the 60-mm collimator, except for the PinPoint chamber and PTW photon diode, all the other detectors showed the same dose buildup (figure 4). These results indicate that shielding in the PTW photon diode and the volume averaging effect in the PinPoint chamber affect the dose buildup of these detectors.

**Analysis of the percentage dose at a 100-mm depth [D<sub>100</sub>]**

The variation in D<sub>100</sub> with eight different detectors was analyzed for all twelve collimators (figure 5). The Scanditronix SFD showed the minimum D<sub>100</sub> values for all collimator sizes except 5 mm. The PTW electron diode showed the minimum D<sub>100</sub> value of 47.15% for the smallest cone, while the PTW PinPoint ion chamber showed the maximum D<sub>100</sub> value of 61.07%. The average D<sub>100</sub>, minimum D<sub>100</sub>, maximum D<sub>100</sub>, and standard deviation of all detectors are tabulated in table 3. The average D<sub>100</sub> was found to be 49.1% ± 1.3% for the smallest collimator (5 mm), whereas the average D<sub>100</sub> was found to be 60.1% ± 0.7% for the largest collimator (60 mm). The standard uncertainty in measurements was found to be within 1% for all collimators.

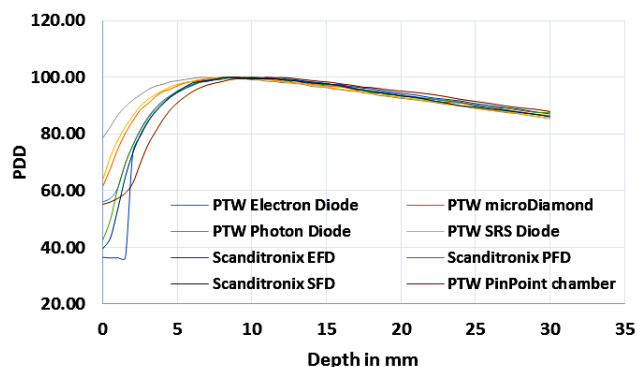


Figure 2. Dose buildup for the 5-mm collimator with different detectors.

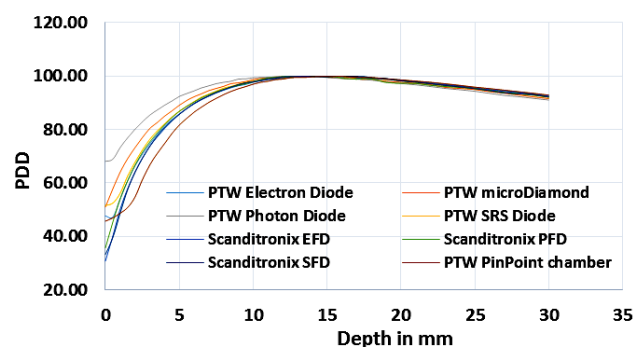


Figure 3. Dose buildup for the 20-mm collimator with different detectors.

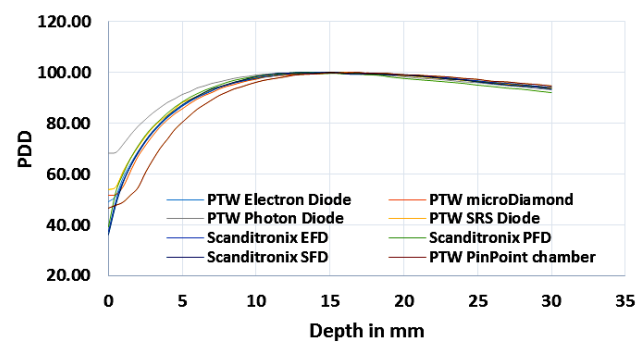
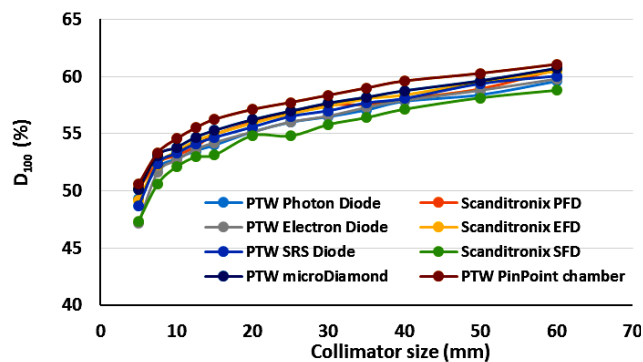


Figure 4. Dose buildup for the 60-mm collimator with different detectors.

Figure 5. Variation in D<sub>100</sub> (%) measured with different detectors for various collimator sizes.



**Table 3.** Average detector response at a 100-mm depth, minimum  $D_{100}$ , maximum  $D_{100}$  and standard deviation of  $D_{100}$  with different detectors for various field sizes.

Collimator Size (mm)	Average $D_{100}$ (%)	Minimum $D_{100}$ (%)	Maximum $D_{100}$ (%)	Maximum-Minimum $D_{100}$ (%)	Standard Deviation $D_{100}$ (%)
5	49.1	47.2	50.6	3.4	1.3
7.5	52.2	50.6	53.3	2.7	0.9
10	53.2	52.1	54.6	2.5	0.7
12.5	54.1	53.0	55.5	2.6	0.8
15	54.7	53.1	56.3	3.1	0.9
20	55.7	54.8	57.1	2.3	0.7
25	56.5	54.8	57.7	2.9	0.9
30	57.1	55.8	58.4	2.6	0.8
35	57.7	56.2	59.0	2.8	0.8
40	58.2	56.6	58.4	1.8	0.7
50	59.1	58.1	60.3	2.2	0.7
60	60.1	58.8	61.1	2.3	0.7

**Analysis of the percentage dose at a 200-mm depth [ $D_{200}$ ]**

The variation in  $D_{200}$  with eight different detectors for all twelve collimators is depicted in figure 6. As expected,  $D_{200}$  showed an increase with the field size with all the detectors. The change in  $D_{200}$  with the field size was appreciable for field sizes from 5 mm to 20 mm, with a maximum difference of 7.60% for the electron diode detector. This deviation was considerably less for field sizes ranging from 30 mm to 60 mm, with the Scanditronix EFD showing a maximum difference of 2.9%. The maximum  $D_{200}$  values were measured using the PTW PinPoint ion chamber for all collimators, whereas the minimum  $D_{200}$  value was obtained using Scanditronix SFD. The average  $D_{200}$ , minimum  $D_{200}$ , maximum  $D_{200}$ , and standard deviation of all detectors are tabulated in table 4. The average  $D_{100}$  was found to be  $22.5\% \pm$

1.1% for the smallest collimator (5 mm) and  $31.3\% \pm 0.7\%$  for the largest collimator (60 mm). The standard uncertainty in measurements was found to be within 1% for all collimators.

**Analysis of the depth of the dose maximum [ $D_{max}$ ]**

An increase in  $D_{max}$  with increasing field size was observed in this study according to the results reported in the literature. However, certain detectors showed a reduced  $D_{max}$  with an increase in the field size. The  $D_{max}$  values obtained with different detectors are shown in figure 7. The PTW photon diode showed the lowest  $D_{max}$  values for all field sizes except for the 60-mm collimator. The PTW PinPoint ion chamber showed larger  $D_{max}$  values for all collimator sizes except for the 20-mm and 25-mm collimators, for which the Scanditronix

**Figure 6.** Variation in  $D_{200}$  (%) measured with different detectors for various collimator sizes.

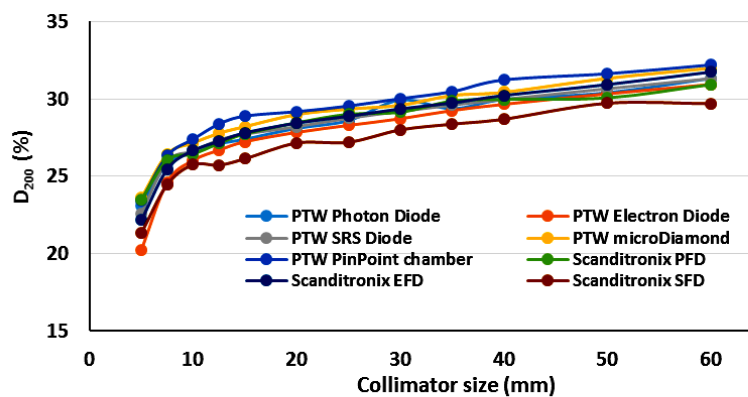


**Table 4.** Average detector response at a 200-mm depth, minimum  $D_{200}$ , maximum  $D_{200}$  and standard deviation of  $D_{200}$  with different detectors for various field sizes.

Collimator Size (mm)	Average $D_{200}$ (%)	Minimum $D_{200}$ (%)	Maximum $D_{200}$ (%)	Maximum-Minimum $D_{200}$ (%)	Standard Deviation $D_{200}$ (%)
5	22.5	20.2	23.6	3.4	1.1
7.5	25.6	24.5	26.4	2.0	0.7
10	26.6	25.7	27.4	1.7	0.5
12.5	27.2	25.7	28.4	2.7	0.7
15	27.6	26.1	28.9	2.8	0.7
20	28.3	27.2	29.2	2.0	0.6
25	28.7	27.2	29.5	2.3	0.7
30	29.2	28.0	30.0	2.0	0.6
35	29.6	28.4	30.5	2.1	0.6
40	30.0	28.7	31.2	2.5	0.7
50	30.6	29.7	31.6	1.9	0.6
60	31.3	29.7	32.2	2.5	0.7

SFD and Scanditronix EFD showed the maximum values. The variation in  $D_{max}$  was observed to be larger for field sizes ranging from 5 mm to 20 mm for all detectors, whereas the variation in  $D_{max}$  was observed to be minimum from 20-mm to 60-mm fields. Figure 8 depicts the average  $D_{max}$ , minimum  $D_{max}$ , maximum  $D_{max}$ , and standard deviation of all detectors. The average

$D_{max}$  value obtained with all detectors was found to be  $9.38 \pm 1.4$  mm for the smallest collimator (5 mm); however, for the largest collimator size of 60 mm, the average  $D_{max}$  value was found to be  $14.91 \pm 1.3$  mm. The depth of the dose maximum value was found to be high in the 40-mm collimator, and the value was noticed to be  $15.19 \pm 0.9$  mm.

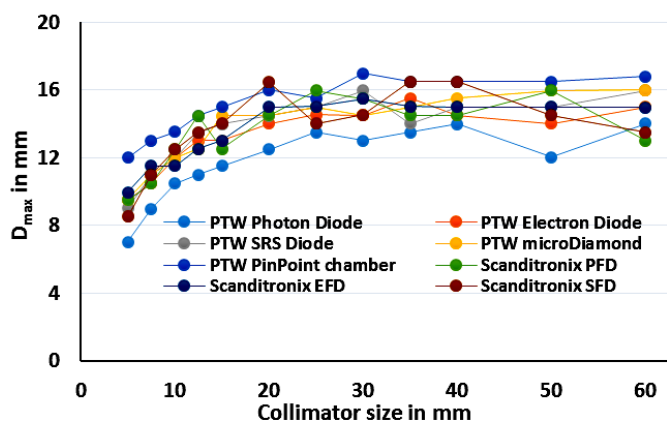


**Figure 7.** Variation in the  $D_{max}$  measured with different detectors for twelve collimators.

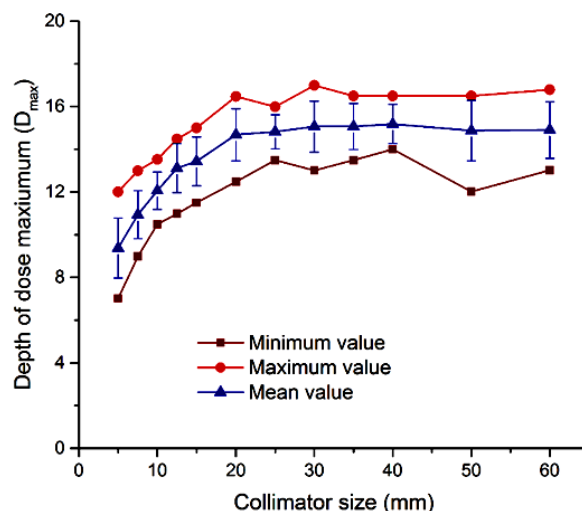


**Figure 8.** Average  $D_{max}$ , minimum  $D_{max}$  and maximum  $D_{max}$  values acquired with all detectors.

**Total scatter factor [ $S_{cp}$ ]**

Figure 9 shows the  $S_{cp}$  at a depth of 10 cm calculated from PDD measurements performed using eight different detectors. Unlike in the conventional linac, there is no  $10 \times 10$  cm field size in the CyberKnife® system; thus, the largest

collimator size of 60 mm is considered as the reference field size. As expected, the  $S_{cp}$  increased with the field size for all eight detectors. For the smallest collimated field of 5 mm, the minimum  $S_{cp}$  value of 0.7887 was observed with the PTW electron diode detector.

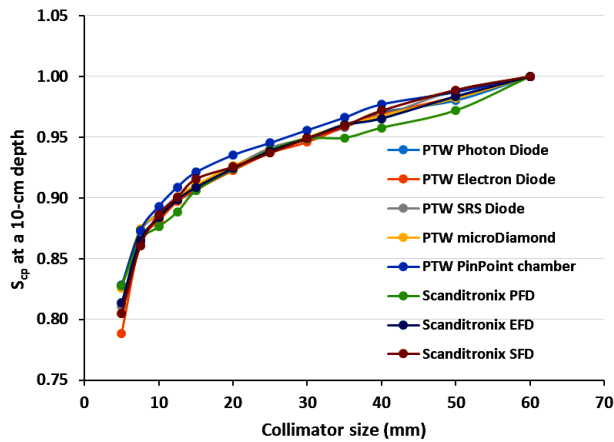


Figure 9. Variation in  $S_{cp}$  at a 10-cm depth using different detectors with various collimator sizes.

A sharp increase in  $S_{cp}$  was observed between 5-mm and 20-mm collimators, while minimal variation was noticed from 25 mm to 60 mm [Fig 9]. For the small fields (5 mm to 20 mm), the maximum variation was observed with the PTW electron diode, with a difference of 16.98%. However, for the larger fields (25 mm to 60 mm), the maximum variation was only 6.71% for the same PTW electron diode and Scanditronix SFD. The differences between the maximum and minimum  $S_{cp}$  values measured using different detectors for all twelve collimators were calculated. The difference was greatest for the 5-mm collimator, with a value of 0.0395 and a standard deviation of 0.0133. However, this difference did not decrease linearly with increasing field size (table 6).

Table 6. Average  $S_{cp}$ , difference between the maximum and minimum  $S_{cp}$  values and standard deviation measured using different detectors with various field sizes.

Collimator size (mm)	Average $S_{cp}$ at 10 cm	Difference between the maximum and minimum $S_{cp}$	Standard deviation
5	0.8159	0.0395	0.0133
7.5	0.8682	0.0139	0.0050
10	0.8851	0.0169	0.0046
12.5	0.8992	0.0205	0.0053
15	0.9107	0.0151	0.0049
20	0.9262	0.0126	0.0036
25	0.9396	0.0082	0.0025
30	0.9496	0.0098	0.0026
35	0.9590	0.0166	0.0043
40	0.9683	0.0192	0.0052
50	0.9833	0.0167	0.0051
60	1.0000	0.0000	0.0000

## DISCUSSION

The uncertainty in the measurement of small-field dosimetric parameters contributes directly to the treatment outcome. We carried out an extensive study using various detectors to investigate the efficacy of detectors in small-field dosimetric measurements. Dosimetric parameters, such as the surface dose, dose buildup, percentage dose at 100 mm and 200 mm, depth of the dose maximum and total scatter factor, were analyzed from the acquired PDD with different detectors. Significant differences in the response of the detectors for small fields were observed in acquired PDD data.

The surface dose indicates the energy spectra because it is mostly due to low-energy components of the radiation beam. The increase in  $D_s$  observed could be due to the scattered photons and extra electron contamination from the treatment head and intervening air column. When the smallest field is used, only a portion of the sensitive volume becomes irradiated at a shallow depth compared with the volume irradiated at a deeper depth due to the divergence of the beam. This irradiation condition results in the higher PDD observed in this study. The surface dose depends on contaminated electrons from the treatment head—i.e., the scattering materials and air along the beam path<sup>(12,13)</sup> and secondary electrons<sup>(12)</sup> produced from the phantom. The  $D_s$  due to contaminant electrons from the head depends on the measurement setup, such as the SSD, field size, and beam-modifying devices along the path<sup>(14)</sup>, and the  $D_s$  due to contaminant electrons from the phantom depends on the field size and measurement setup. Many studies have been carried out on  $D_s$  measurements using different detectors, such as those using a thermo luminescence dosimeter<sup>(16)</sup>, radiochromic film<sup>(17)</sup>, parallel-plate ionization chambers<sup>(18)</sup> and semiconductor detectors. Although the thimble ion chambers and semiconductor diodes are not indicated to measure  $D_s$ , especially in small fields, a comparative analysis of  $D_s$  using various detectors and the significance of the field size was performed. The  $D_s$  measured using the PTW

microDiamond showed higher values than those measured using other detectors. The over-response of the microDiamond detector could be due to its higher mass density ( $3.5 \text{ g cm}^{-3}$ ) although it has a mass energy absorption coefficient similar to that of water<sup>(17)</sup>. Our study and many others have demonstrated the microDiamond over responding at smaller field sizes. The increase in  $D_s$  observed could be due to the scattered photons and extra electron contamination from the treatment head and intervening air column<sup>(20, 27, 28)</sup>. McCullough analyzed the significance of the dose buildup in the dose prescription from the acquired central axis depth dose curves<sup>(18)</sup>. A huge difference was noted in the dose buildup for a small collimator size of 5 mm between different detectors. This could be due to the gradient in the flux or charge particle equilibrium in different detectors that is prominent in very small field sizes. In diodes, the size of the active chip and quantity of the surrounding epoxy material also play a major role in the dose buildup for small collimator sizes.

The change in the PDD values at a 100-cm depth is due to variations in the scattering of electrons and photons from the collimator and phantom<sup>(19)</sup>. The PTW PinPoint chamber showed a maximum  $D_{100}$  for all collimator sizes due to the volume averaging effect<sup>(20, 21)</sup>. For smaller collimator sizes, only a part of the ion chamber was irradiated at shallow depths; hence, the volume averaging effect decreased with depth due to divergence of the beam. Buccioli reported that ion chambers show larger doses than diode detectors, a finding that is in agreement with our measurements<sup>(22)</sup>. The PTW microDiamond was observed to over respond in small fields. A small error in detector positioning can cause significant error in the depth dose measurement in small fields<sup>(23)</sup>. The PDD values were observed to increase with the field size at the 20-cm depth for all detectors. A similar result was observed by Aspradakis *et al.*, in which the PDD values increased with the field size<sup>(24)</sup>. Errors in positioning of the detector to the central axis of the beam influence the PDD measurements<sup>(25)</sup>. These changes in PDD values are due to the variation in the scattering of

electrons and photons from the collimator and phantom, respectively.

The depth of the dose maximum ( $D_{\text{max}}$ ) is an important parameter in the dose distribution along the central axis and is dependent on the beam energy, field size, and SSD. Theoretically, for a given beam energy,  $D_{\text{max}}$  increases rapidly with increasing field size, reaching its peak at a field size of  $5 \times 5 \text{ cm}^2$ , and then decreases with further increases in the field size<sup>(26)</sup>. The PTW photon diode has shown the lowest  $D_{\text{max}}$  values for all field sizes except for the 60-mm collimator. In the design of the shielded diode, due to the presence of high atomic material, a low-energy scatter can be absorbed that may lead to the under-response of the detector<sup>(31)</sup>. Shukaili reported that the large variation in the  $D_{\text{max}}$  value using different detectors with various field sizes could be mainly due to the nonequilibrium condition that is dependent on the type and design of the detector<sup>(27)</sup>. As noted by Das, smaller fields produce challenges in dose measurements with greater chances of a significant error<sup>(28)</sup>. The difference noticed between PFD and EFD at  $D_{\text{max}}$  could be due to the differences in the response of the detectors to contaminant electrons and was also noticed by Das *et al.*<sup>(28)</sup>.

The  $S_{\text{cp}}$  depends on the field size, SSD, depth of measurement, type of beam collimation and detector used for measurement. The  $S_{\text{cp}}$  is defined as the ratio of the dose in water for a given field size at the reference depth  $d$  to the dose at the same point for the reference field size<sup>(28)</sup>. Because  $S_{\text{cp}}$  is a function of field size, as the field size increases, not only the primary radiation increase but also the number of scattered radiation increases. This increase will only result in a higher level of ionization, and thus a higher dose, measured by the detectors. The difference in the output factor measured using different detectors was found to be high for the smallest field, as reported in the literature<sup>(32)</sup>. This difference infers that the density of the detector becomes important as the lateral electronic disequilibrium breaks down considerably at very small field sizes<sup>(17, 31)</sup>. The rapid decrease in the primary dose where electronic equilibrium does not exist in

fields smaller than the lateral electron range could be due to the observed field size dependency of the output factor.

## CONCLUSION

We investigated different detectors to determine the effectiveness of each detector in the dosimetric measurements of small fields. Quantification of the deviations and differences in the  $D_s$ , dose buildup,  $D_{100}$ ,  $D_{200}$ ,  $D_{max}$  and  $S_{cp}$  provides a better understanding of the potential outcomes of these parameters and their influence on the dose prescription and treatment delivery. Being cautious in the selection of a detector and understanding the detector's characteristics and limitations are required before using it in small-field dosimetry. We conclude that the selection of an appropriate detector in a small field is crucial for accurate measurements that, in turn, affects the dose delivery. New protocols for small-field dosimetry for accurate dose calculation are promising but address the absorbed dose determination in nonequilibrium conditions. Further studies with Monte Carlo simulation would eliminate the experimental uncertainties and accurately determine the small-field dosimetric parameters.

## ACKNOWLEDGEMENTS

The authors like to thank Ms. Retna Ponmalar of Christian Medical College at Vellore, India for her valuable suggestions to this paper. The authors would also like to thank Mr. B. Viswanathan of PTW Dosimetry India for the guidance, encouragement and financial assistance for this research work.

**Conflicts of interest:** Declared none.

## REFERENCES

1. Guthrie BL and Adler JR Jr. (1992) Computer-assisted pre-operative planning, interactive surgery, and frameless

- stereotaxy. *Clin Neurosurg*, **38**: 112-131.
2. Echner GG, Kilby W, Lee M, Earnst E, Sayeh S, Schlaefer A, et al. (2009) The design, physical properties and clinical utility of an iris collimator for robotic radiosurgery. *Phys Med Biol*, **54**: 5359-5380.
3. Das IJ, Ding GX, Ahnesjö A (2008) Small fields: Nonequilibrium radiation Dosimetry. *Med Phys*, **35(1)**: 206-215.
4. Seuntjens J and Verhaegen F (2003) Ionization chamber dosimetry of small photon fields: A Monte Carlo Study on stopping-power ratios for radiosurgery and IMRT beams. *Physics in Medicine and Biology*, **48(21)**.
5. Yarahmadi M, Nedaie HA, Allahverdi M, Asnaashar Kh, Sauer OA (2013) Small photon field dosimetry using EBT2 Gafchromic film and Monte Carlo simulation. *Int J Radiat Res*, **11(4)**: 215-224.
6. Report of AAPM TG 135. (2011) Quality assurance for robotic radiosurgery. *Med Phys*, **38(6)**: 2914-36.
7. Morales JE, Crowe SB, Hill R, Freeman N, Trapp JV (2016) Dosimetry of cone-defined stereotactic radiosurgery fields with a commercial synthetic diamond detector. *Medical Physics*, **41**: 111702-1.
8. Masi L, Russo S, Francescon P, Doro R, Frassanito MC, Fumagalli ML, et al. (2016) CyberKnife beam output factor measurements: A multi-site and multi-detector study. *Physica Medica*, **32(12)**: 1637-1643.
9. Sharma S (2014) Challenges of small photon field dosimetry are still challenging. *Journal of Medical Physics*, **39(3)**: 131.
10. Keivan H, Shahbazi-Gahrouei D, Shanei A (2018) Evaluation of dosimetric characteristics of diodes and ionization chambers in small megavoltage photon field dosimetry. *Int J Radiat Res*, **16(3)**: 311-321.
11. Pappas E, Maris TG, Zacharopoulos F, Papadakis A, Manolopoulos S, Green, et al. (2008) Small SRS photon field profile dosimetry performed using a PinPoint air ion chamber, a diamond detector, a novel silicon-diode array (DOSI), and polymer gel dosimetry. Analysis and inter-comparison. *Med Phys*, **35(10)**: 4640-8.
12. Ling CC and Biggs PJ (1979) Improving the buildup and depth-dose characteristics of high energy photon beams by using electron filters. *Med Phys*, **6**: 296-301.
13. Mc Parland BJ (1991) The effects of a universal wedge and beam obliquity upon the central axis dose buildup for 6-MV X-rays. *Med Phys*, **18**: 740-743.
14. Nilsson B and Sorcini B (1989) Surface dose measurements in clinical photon beams. *Acta Oncol*, **28**: 537-442.
15. Lamb A and Blake S (1998) Investigation and modelling of the surface dose from linear accelerator produced 6 and 10 MV photon beams. *Phys Med Biol*, **43**: 1133-1146.
16. Devic S, Seuntjens J, Abdel-Rahman W, Evans M, Olivares M, Podgorsak EB, et al. (2006) Accurate skin dose measurements using radiochromic film in clinical applications. *Med Phys*, **33**: 1116.
17. Scott AJD, Kumar S, Nahum AE, Fenwick JD (2012) Characterizing the influence of detector density on dosimeter response in non-equilibrium small photon fields. *Phys Med Biol*, **57(14)**: 4461-4476.

18. McCullough EC (1994) A measurement and analysis of buildup region dose for open field photon beams (cobalt-60 through 24 MV). *Med Dosim*, **19**: 5–14.
19. Ding GX and Ding F (2012) Beam characteristics and stopping-power ratios of small radiosurgery photon beams. *Phys Med Biol*, **57**: 5509-5521.
20. Heydariyan M, Hoban PW, Beddoe AH (1996) A comparison of dosimetry techniques in stereotactic radiosurgery. *Phys Med Biol*, **41**: 93-110.
21. Wilcox EE and Daskalov GM (2007) Evaluation of GAF-CHROMIC EBT film for Cyberknife dosimetry. *Med Phys*, **34**: 1967-1974.
22. Bucciolini M, Buonamici FB, Mazzocchi S, De Angelis C, Onori S, Cirrone GA (2003) Diamond detector versus silicon diode and ion chamber in photon beams. *Med Phys*, **30(8)**: 2149-2154.
23. Marsolat F, Tromson D, Tranchant N, Pomorski M, Le Roy M, Donois M, et al. (2013) A new single crystal diamond dosimeter for small beam: Comparison with different commercial active detectors. *Phys Med Biol*, **58**: 7647-7660.
24. Aspradakis MM, Byrne JP, Palmans H, Duane S, Conway J, Warrington AP, et al. (2010) IPEM Report Number 103: Small Field MV Photon Dosimetry. Book of Extended Synopses.
25. Godson HF, Ravikumar M, Sathiyam S, Ganesh KM, Retna Ponmalar Y, Varatharaj C (2016) Analysis of small field percent depth dose and profiles: Comparison of measurements with various detectors and effects of detector orientation with different jaw settings. *J Med Phys*, **41(1)**: 12–20.
26. Marsolat F, Tromson D, Tranchant N, Pomorski M, Le Roy M, Donois M, et al. (2013) A new single crystal diamond dosimeter for small beam: comparison with different commercial active detectors. *Phys Med Biol*, **58(21)**: 7647-7660.
27. Podgorsak EB (2005) Vienna: International Atomic Energy Agency; Radiation Oncology Physics: A Handbook for Teachers and Students.
28. Al Shukaili K, Petasecca M, Newall M, Espinoza A, Pervertaylo VL, Corde S, et al. (2017) A 2D silicon detector array for quality assurance in small field dosimetry. *Medical Physics*, **44**: 628-636.
29. Das IJ, Ding GX, Ahnesjö A (2008) Small fields: Nonequilibrium radiation Dosimetry. *Med Phys*, **35(1)**: 206-215.
30. McCullough EC (1994) A measurement and analysis of buildup region dose for open field photon beams (cobalt-60 through 24 MV). *Med Dosim*, **19(1)**: 5-14.
31. Podgorsak EB (2005) Radiation Oncology Physics: A Handbook for Teachers and Students. International Atomic Energy Agency, Vienna.
32. Godson HF, Ravikumar M, Sathiyam S, Ganesh KM, Ponmalar YR, Varatharaj C (2016) Analysis of small field percent depth dose and profiles: Comparison of measurements with various detectors and effects of detector orientation with different jaw settings. *J Med Phys*, **41(1)**: 12–20.

